4-16-2018

Ice Core Records of West Greenland Melt and Climate Forcing

H.P. Marshall
Boise State University

T. Meehan
Boise State University

Geophysical Research Letters

RESEARCH LETTER
10.1002/2017GL076641

Key Points:
- Ice cores from the West Greenland percolation zone confirm a significant increase in surface melt rates since the early 1990s
- Modern melt rates in West Greenland are unmatched in a composite ice core melt record back to 1550 CE
- Greenland blocking, regional sea surface temperatures, and a long-term summer warming trend are required to explain modern melt rates

Supporting Information:
- Supporting Information S1
- Figure S1
- Figure S2
- Figure S3
- Figure S4
- Figure S5

Correspondence to:
K. A. Graeter and E. C. Osterberg,
karinagraeter@gmail.com;
erich.c.osterberg@dartmouth.edu

Citation:
Graeter, K. A., Osterberg, E. C., Ferris, D. G., Hawley, R. L., Marshall, H. P., Lewis, G., et al. (2018). Ice core records of West Greenland melt and climate forcing. *Geophysical Research Letters*, *45*, 3164–3172. https://doi.org/10.1002/2017GL076641

Received 2 DEC 2017
Accepted 17 MAR 2018
Accepted article online 26 MAR 2018
Published online 6 APR 2018

Ice Core Records of West Greenland Melt and Climate Forcing

K. A. Graeter[1], E. C. Osterberg[1], D. G. Ferris[1], R. L. Hawley[1], H. P. Marshall[2], G. Lewis[1], T. Meehan[2], F. McCarthy[3], T. Overly[1], and S. D. Birkel[4]

[1]Department of Earth Sciences, Dartmouth College, Hanover, NH, USA, [2]Department of Geosciences, Boise State University, Boise, ID, USA, [3]College of Fisheries and Ocean Sciences, University of Alaska Fairbanks, Fairbanks, AK, USA, [4]Climate Change Institute and School of Earth and Climate Sciences, University of Maine, Orono, ME, USA

Abstract Remote sensing observations and climate models indicate that the Greenland Ice Sheet (GrIS) has been losing mass since the late 1990s, mostly due to enhanced surface melting from rising summer temperatures. However, in situ observational records of GrIS melt rates over recent decades are rare. Here we develop a record of frozen meltwater in the west GrIS percolation zone preserved in seven firn cores. Quantifying ice layer distribution as a melt feature percentage (MFP), we find significant increases in MFP in the southernmost five cores over the past 50 years to unprecedented modern levels (since 1550 CE). Annual to decadal changes in summer temperatures and MFP are closely tied to changes in Greenland summer blocking activity and North Atlantic sea surface temperatures since 1870. However, summer warming of ~1.2°C since 1870–1900, in addition to warming attributable to recent sea surface temperature and blocking variability, is a critical driver of high modern MFP levels.

Plain Language Summary Computer models and satellites show that the amount of snow melting each summer on Greenland has increased since the 1990s, but it is difficult to confirm this directly on the ice sheet. When surface snow melts, the water spreads into deeper layers of snow and refreezes as an ice layer. As fresh snow buries each summer's ice layers, the history of snowmelt is preserved in the ice sheet. We describe seven ice cores collected from western Greenland that contain the history of ice layers back to 1966. We find more ice layers, caused by more summer melting, since the 1990s. By comparing our ice cores to a longer ice core from the same area, we show that today's melt rates are the highest in this region since at least 1550 CE. Year-to-year changes in the amount of melting are mostly caused by changes in the number of summer high-pressure systems and fluctuating ocean temperatures near Greenland. Although both of these processes have contributed to recent high melt rates, Greenland is 1.2°C warmer today than during similar conditions in the 1890s. This "extra" warming is most likely caused by human greenhouse gas emissions, leading to the unusual melt rates of recent years.

1. Introduction

The Greenland Ice Sheet (GrIS) has been losing mass since at least 1998, contributing approximately 0.7 mm/year to global sea level rise (van den Broeke et al., 2016). Although ice discharge is a major contributor to GrIS mass loss, most of the loss since the early 2000s is due to enhanced surface melt and runoff (Enderlin et al., 2014). As GrIS air temperatures warm in response to higher greenhouse gas concentrations, surface melt is expected to increase (Fettweis et al., 2013), contributing up to 13 cm of sea level rise by 2100 (Church et al., 2013). Over the last 20 years, the fastest warming rates (Hanna et al., 2012) and surface mass balance loss (Sasgen et al., 2012) have occurred in West Greenland.

While the recent increase in GrIS surface melt has been observed by remote sensing (Mote, 2007; Tedesco et al., 2013) and predicted by surface mass balance models (e.g., Box et al., 2006; Fettweis et al., 2016), direct observations of recent surface melt are comparatively rare. Approximately 40% of all surface meltwater generated on the GrIS percolates vertically through the snowpack and refreezes in the firn pore space (van Angelen et al., 2013). Much of this refreezing takes place in the percolation zone, a large region of the GrIS bounded by the equilibrium line altitude at its lowest elevations and the dry snow line at its highest (Benson, 1962). Thus, temporal trends in surface melt are recorded by the amount of meltwater refreeze within the percolation zone and can be sampled by firn and ice cores. The Program for Arctic Regional Climate Assessment (PARCA) collected and dated a series of firn cores from the GrIS percolation zone in 1997–1998 (Mosley-Thompson et al., 2001), prior to the high melt years of the 2000s and early 2010s (e.g., Nghiem et al., 2012). Recent field campaigns have examined shallow firn cores to

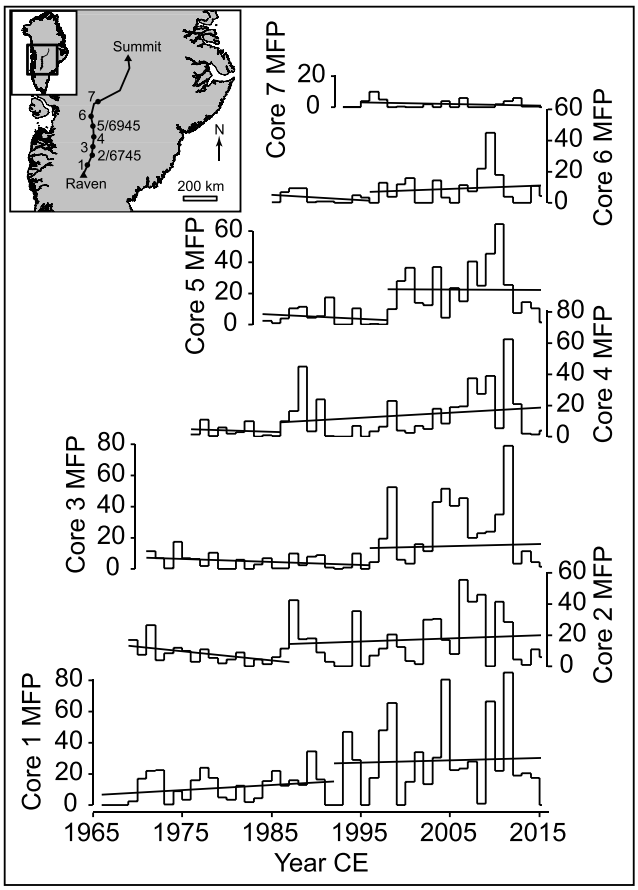

Figure 1. Melt feature percent (MFP) records from GreenTrACS firn cores (numbered points on inset map) collected along a traverse (black line on inset map) across the West Greenland percolation zone. Significant increases in MFP identified by Pruned Exact Linear Time changepoint analysis are represented by breaks in trend lines.

investigate the regional and year-to-year variability of meltwater refreeze (De la Peña et al., 2015; Machguth et al., 2016). However, without depth-age relationships, it is difficult to confirm temporal relationships between surface meltwater generation and climate forcing from these records.

Here we present a study of ice layers preserved in seven firn cores collected in 2016 from a broad region of the west GrIS percolation zone (2,100–2,500 m elevation) as part of the Greenland Traverse for Accumulation and Climate Studies (GreenTrACS; Figure 1 and Table S1 in the supporting information). We develop records of annual accumulation and refrozen meltwater distribution to calculate the annual melt feature percentage (MFP) over the past 50 years. We extend the west GrIS melt record to 1547 CE by combining our GreenTrACS MFP record with that from a previously collected ice core, Site J, located within our study area (Kameda et al., 1995). We also quantify changes in near-surface firn density from 1998 to 2016 though comparison of colocated GreenTrACS and PARCA cores.

Previous researchers have associated the recent increase in GrIS surface melt with warmer North Atlantic sea surface temperatures (SSTs) and an increased frequency of summer blocking anticyclones over Greenland (Fettweis et al., 2013; Hanna, Jones, et al., 2013; McLeod & Mote, 2015; Mote, 1998). Our analysis supports the importance of Greenland blocking and regional SSTs in driving multidecadal GrIS melt rates, but we find that an additional warming component is required to explain the anomalous melt features since the 1990s.

2. Data and Methods

We collected seven shallow (22–31 m long) firn cores from the percolation zone of the west GrIS during May–June 2016 along an 830-km snowmobile traverse from Raven (Dye 2) to Summit station (inset in Figure 1 and Table S1). The firn cores were drilled using an Ice Drilling and Design Office hand auger with a Kyne sidewinder attachment. Core sites 1–6 are located approximately 65 km from one another along the traverse route that roughly follows the 2,160 m above sea level elevation contour. Core site 7 is at 2,462 m elevation along the Expéditions Glaciologiques Internationales au Groenland line. Core sites 2 and 5 reoccupy the 1998 PARCA core sites 6745 and 6945, respectively (Mosley-Thompson et al., 2001).

We measured the mass, length, and diameter of 0.03–1 m firn core segments to calculate density. The firn cores were sampled for chemical measurements using a continuous ice core melter system with discrete sampling in the Dartmouth College Ice Core Laboratory (Osterberg et al., 2006). An Abakus (Klotz) laser particle detector continuously measured microparticle concentrations directly from the ice core meltwater stream. We measured major ion (Na^+, NH^{4+}, K^+, Mg^{2+}, Ca^{2+}, Cl^-, NO_3^-, and SO_4^{2-}) and methanesulphonic acid concentrations using a Dionex Model ICS5000 capillary ion chromatograph. We measured oxygen isotope ratios ($\delta^{18}O$, δD) using a Picarro L1102-I and a Los Gatos Research Liquid Water Isotope Analyzer. The sample size was approximately 0.05 water-equivalent meters for all cores.

We determined depth-age curves by identifying annual layers based on robust seasonal oscillations in $\delta^{18}O$ and the concentrations of major ions, methanesulphonic acid, and dust, consistent with previous ice core studies (Figure S1; Mosley-Thompson et al., 2001; Osterberg et al., 2015). We combined the depth-age curves with core density to calculate annual accumulation rates.

To measure the total amount of meltwater refrozen as ice layers, we used a light table to measure the thickness of the ice layers in each core. We analyzed ice layers rather than wetted firn because piping and ice layer formation, rather than the propagation of a uniform wetting front, is the dominant mode of meltwater refreeze at these elevations (Pfeffer & Humphrey, 1998). As this region is above the runoff line, we assume that all

surface meltwater refreezes within the firn. We limit our analysis only to ice layers that extend the entire width of the core. Each individual ice layer may not be spatially extensive (Benson, 1962), but we assume that the larger trends of ice layers within each core are a representative sample of the ice layers present in the local firn.

The total thickness of ice layers within a given year's annual layer was calculated to determine each annual ice layer thickness. Ice layers located within a given year of firn may not have been generated during that year, or even during the following year, as meltwater typically percolates to depths greater than 1 m (Benson, 1962; Cox et al., 2015; Harper et al., 2012). However, measuring the total ice layer thickness by year establishes a time series with which we may identify patterns and determine long-term trends in surface melt.

MFP was calculated by dividing the annual ice layer thickness in water-equivalent meters by the annual accumulation. An ice layer consists of not only surface meltwater refrozen at depth but also firn melted during vertical percolation and firn melted at the depth of ice layer formation. Thus, a single ice layer may consist of melted snow or firn from one or more years, depending on the depth of percolation. Ice layers therefore represent total melt effects, rather than a direct measurement of melt at the surface.

We use the Pruned Exact Linear Time (PELT) changepoint analysis (Killick et al., 2012) to identify abrupt and significant shifts in the mean or slope of the MFP records. For our MFP trend analyses, we exclude the year 2016 because the GreenTrACS cores were collected in May and early June, before the onset of widespread melt at these elevations. We also exclude 2015 because observations of meltwater percolation and refreeze in the West Greenland percolation zone indicate that meltwater typically penetrates to >1 m depth (Braithwaite et al., 1994; Cox et al., 2015; Humphrey et al., 2012). Therefore, it is likely that the 2015 annual layer in our 2016 cores has not been subjected to a similar level of meltwater percolation and refreeze as the deeper firn.

We evaluate relationships among west GrIS MFP, west GrIS temperature, 500 mb Greenland blocking, and North Atlantic SSTs using output from the Modèle Atmosphérique Régional (MARv3.7; Fettweis et al., 2016) and the twentieth century reanalysis model (Compo et al., 2011). We also compare against the Danish Meteorological Institute temperature record from Nuuk (Cappelen, 2015), located ~500 km south of our study area.

3. Results

3.1. Temporal Changes in Melt Feature Percent

Cores 1–5 show statistically significant increases in MFP toward present (linear regression, $p < 0.05$), with the largest increase observed in Core 5 (0.94%/year; Figure 1). There is a small but insignificant ($p > 0.05$) increase in MFP in Core 6 and no significant trend in Core 7. The lack of any trend at Core 7 is consistent with its significantly higher latitude and elevation.

PELT changepoint analysis highlights the recent increase in surface melt, identifying significant positive shifts in MFP ranging from 1992 to 1998 in Cores 1, 3, 5, and 6 and from 1986 to 1987 in Cores 2 and 4 (Figure 1). The increases in MFP identified in the GreenTrACS cores is generally consistent with surface mass balance estimates of increased melt starting in the early 1990s (Burgess et al., 2010; van Angelen et al., 2014; van den Broeke et al., 2016), accounting for variable percolation into older firn layers.

While Cores 1–5 show significant increases in meltwater refreeze toward present, the detailed temporal distribution of MFP differs between cores. Multiyear differences in MFP changepoints at adjacent cores (e.g., 1987 in Core 2 and 1996 in Core 3) are unlikely to represent real differences in surface temperature forcing given that they are spaced only ~65 km apart. There is no trend in annual accumulation in any of the cores (not shown), precluding a significant effect on MFP trends. Neither changepoint years nor changepoint depths correlate with differences in the cores' mean annual accumulation. Rather, these stratigraphic differences in MFP highlight the complex, heterogenous nature of meltwater percolation and refreezing (Benson, 1962; Cox et al., 2015; Pfeffer & Humphrey, 1998) and indicate that MFP time series should be interpreted on a multiannual to decadal scale.

3.2. Impact of Meltwater Percolation on Firn Density

We quantify changes in firn density since 1998 by calculating differences between colocated GreenTrACS and PARCA core densities at common depths. A paired, nonparametric sign test indicates that GreenTrACS Cores 2 and 5 have significantly higher density than the colocated PARCA Cores 6745 ($p < 0.05$) and 6945 ($p < 0.05$),

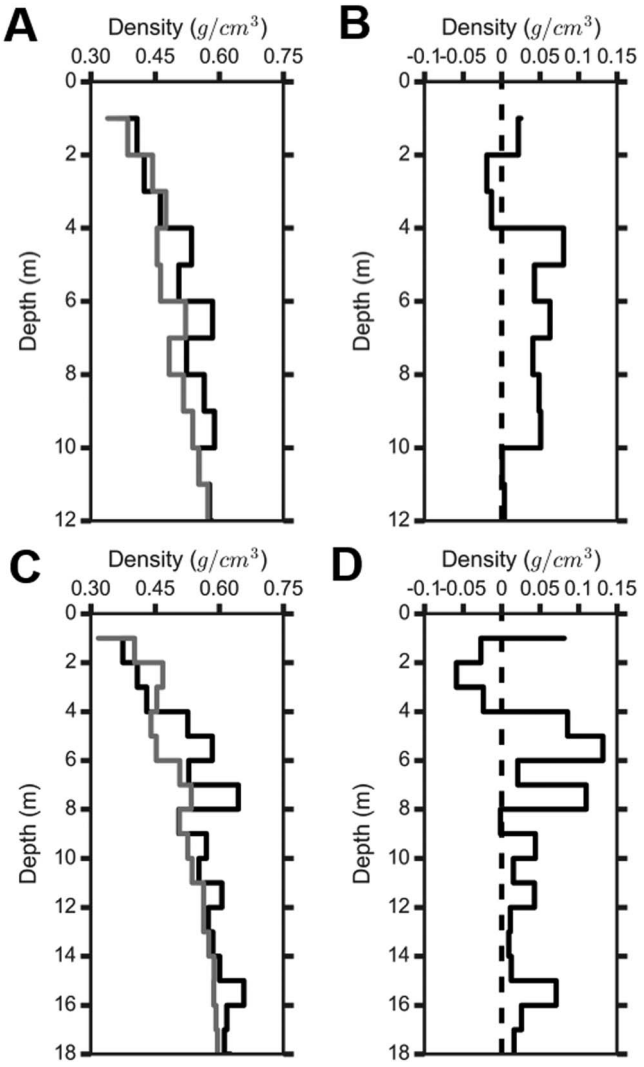

Figure 2. (a) Density comparison between colocated ice cores Greenland Traverse for Accumulation and Climate Studies Core 2 (black line) and Program for Arctic Regional Climate Assessment Core 6745 (gray line), and (b) their density difference at common depths. (c and d) Same as (a) and (b), except for colocated Greenland Traverse for Accumulation and Climate Studies Core 5 (black) and Program for Arctic Regional Climate Assessment Core 6945 (gray).

respectively (Figure 2). The average increase in density from 1 to 12 m depth is 8.0% at Core 2 and 11.3% at Core 5. Density increases in Cores 2 and 5 correlate strongly with total ice layer thickness by meter (Core 2: $r = 0.85$ and $p < 0.01$; Core 5: $r = 0.81$ and $p < 0.001$), confirming that the increase in firn density is primarily related to higher MFP in recent decades. This significant increase in firn density highlights the importance of including deep meltwater percolation in altimetry-based mass balance measurements, which require firn density estimates to derive mass change from surface elevation change (Li & Zwally, 2011; Sørensen et al., 2011).

3.3. Extending the MFP Record to 1547 CE

To provide a longer context for the recent increase in MFP, we combine our GreenTrACS MFP record from Core 1 with the Site J ice core MFP record (Kameda et al., 1995; Figure 3a). Site J is located 29 km from Core 1 and 100 m lower in elevation (66°51.9′N, 46°15.9′W, 2030 m above sea level). The Site J MFP record extends from 1547 to 1989 CE, providing 24 years of overlap with Core 1 (1966–1989). We regress the MFP time series from the two cores over 1966–1989 and convert the Core 1 MFP record to Site J equivalent MFP using the regression equation ($MFP_{Site\_J} = 0.81 * MFP_{GTC\_1} + 16.5$). The combined west GrIS ice core MFP record shows that the recent increase in MFP is unmatched back to 1547 CE (Figures 3a and S2).

3.4. Climate Drivers of West Greenland Temperature and MFP

Figure 3 shows that the recent increase in west GrIS MFP (Figure 3a) parallels the rise in regional summertime (June–August; hereafter "JJA") temperatures. We compare the MFP record to MARv3.7 model output from the Core 6 location (Figure 3b; hereafter "Core 6 JJA temperature") and to JJA mean temperature observations from Nuuk (Figure 3c). The period since 2000 CE is the warmest of both records, consistent with the highest MFP of the record over the same interval ($MFP_{2000–2014} = 42.3\%$). However, the Nuuk record shows that JJA temperatures have only recently exceeded the warmth of the 1930s to 1940s (Figure 3c), an observation consistent with other long-term instrumental temperature records in western coastal Greenland (Mernild et al., 2014). Interestingly, the Site J record shows relatively elevated melt from 1947 to 1961 ($MFP_{1947–1961} = 25.9\%$) but comparatively low MFP in the 1930s and most of the 1940s ($MFP_{1930–1946} = 13.5\%$). The low MFP values during the warmest decade of the twentieth century in western Greenland (the 1930s) are currently unexplained and warrant future examination.

To examine the influence of ocean and atmospheric circulation on West Greenland summer temperature and MFP, we spatially correlated Core 6 JJA temperatures with North Atlantic JJA SSTs (Figure 4a) and with JJA 500 mb geopotential height (Z_{500}; Figure 4b) from the twentieth century reanalysis model (Compo et al., 2011). The correlation patterns in Figure 4 are insensitive to which ice core site is chosen for MARv3.7 temperatures. Core 6 JJA temperature is significantly and positively correlated ($p < 0.05$) with SSTs in the Denmark Strait south of Iceland and across a broad region of the tropical Atlantic (Figure 4a). This supports a link between warmer Denmark Straight SSTs and enhanced melt on the west GrIS. The spatial correlation pattern is similar to the canonical Atlantic Multidecadal Oscillation (AMO) pattern, a 60–70 year pattern of North Atlantic SST variability (Kerr, 2000), except that the GrIS correlations are stronger in the North Atlantic while the AMO correlations are stronger in the tropics (Figure S3). The Denmark Strait summer SST time series is significantly correlated with the summer AMO index from 1871 to 2015 ($r = 0.63$, $p < 0.001$).

Core 6 JJA temperatures are also strongly and positively correlated ($p < 0.05$) with Z_{500} centered over the Denmark Strait (Figure 4b). High Denmark Straight Z_{500} is indicative of more frequent Greenland blocking,

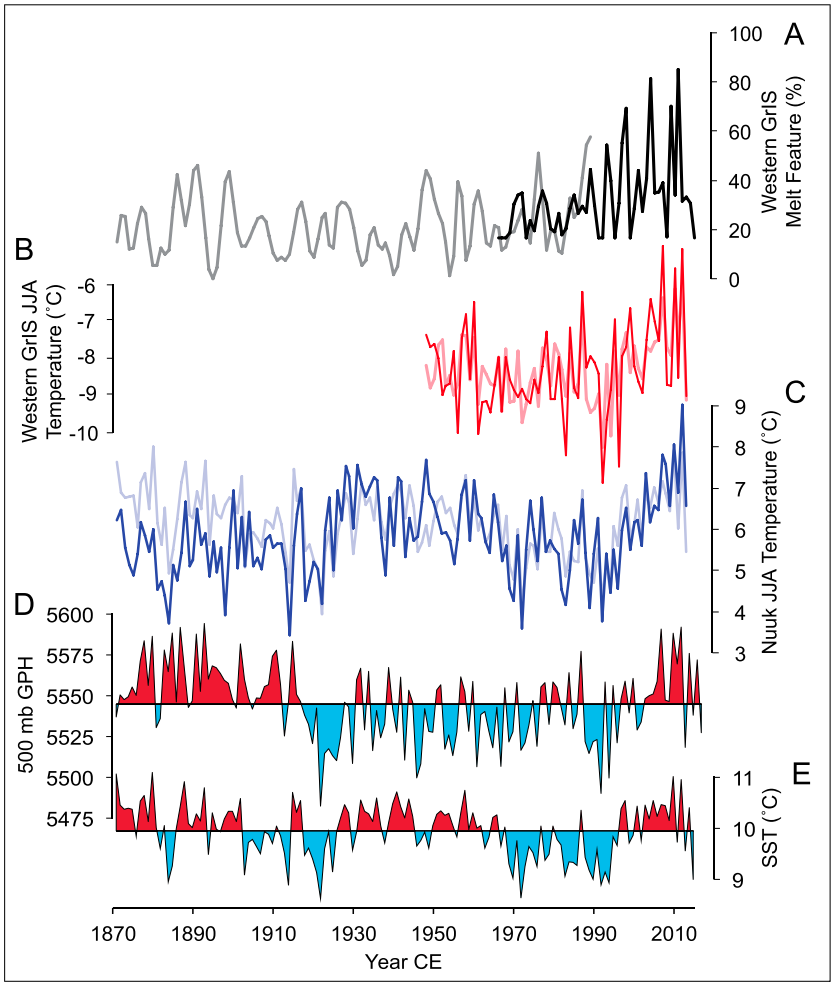

Figure 3. Comparison of ice core melt feature percentage (MFP), regional temperature, and atmospheric circulation records since 1871. (a) Greenland Traverse for Accumulation and Climate Studies Core 1 MFP record (black curve), adjusted through regression (see text) to be consistent with the nearby Site J MFP record (gray curve) during their period of overlap (1966–1989). (b) West Greenland Ice Sheet (GrIS) summer (June–August, JJA) temperature at Core 6 from the Modèle Atmosphérique Régional climate model (red curve) and a multilinear regression west GrIS JJA temperature model using the Denmark Strait Z_{500} and sea surface temperature (SST) records displayed in (d) and (e) (pink curve). (c) JJA temperature recorded at Nuuk, Greenland (dark blue curve) and a multilinear regression Nuuk JJA temperature model using the Denmark Strait Z_{500} and SST records displayed in (d) and (e) (light blue curve). (d) The 500 mb geopotential height (Z_{500}) from twentieth century reanalysis data (Compo et al., 2011) averaged over the Denmark Strait region of highest correlation (boxed region in Figure 4b). (e) JJA SSTs from twentieth century reanalysis data averaged over the Denmark Strait region of highest correlation (boxed region in Figure 4a).

where a high-pressure anomaly centered off the SE coast of Greenland strengthens anticyclonic southwesterly winds over West Greenland, increasing temperatures over the west GrIS through the advection of warm southerly air (Hanna, Navarro, et al., 2013; Mote, 1998). This blocking pattern is shifted to the southeast relative to the Greenland Blocking Index (GBI) of Hanna et al. (2012; Figure S4), although the time series of Denmark Strait summer Z_{500} is highly correlated with the summer GBI ($r = 0.73$, $p < 0.001$).

The strong influence of Greenland blocking and North Atlantic SSTs on multidecadal west GrIS temperatures and melt rates is apparent in time series in Figure 3. The recent period of anomalously warm temperatures and high MFP coincides with elevated Denmark Strait Z_{500} (Figure 3d), indicative of frequent summer blocking, and with warm Denmark Strait SSTs (Figure 3e). Two earlier periods of relatively high MFP from 1947 to 1961 ($MFP_{1947–1961} = 25.9\%$) and 1885 to 1900 ($MFP_{1885–1900} = 27.5\%$) also occur during periods of warm SSTs (Figure 3e). The 1885–1900 period was also associated with more frequent summer blocking (Figure 3d). Thus,

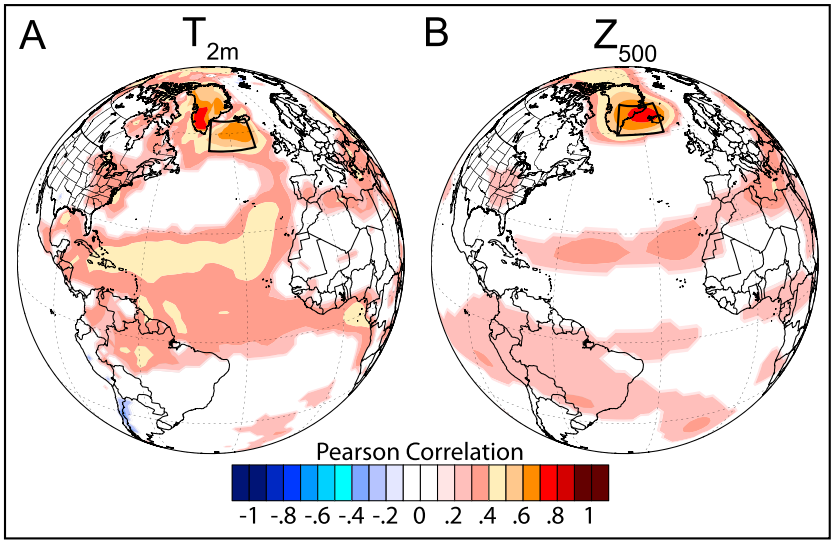

Figure 4. Spatial correlations from 1948 to 2012 between Modèle Atmosphérique Régional June–August surface temperatures at Core 6 and twentieth century reanalysis (Compo et al., 2011) 2 m temperature (T_{2m}; a) and 500 mb geopotential height (Z_{500}; b). Only statistically significant correlations ($p < 0.05$) are displayed. Boxed regions represent the areas of strongest correlation over the Denmark Strait. Images obtained using Climate Reanalyzer (http://cci-reanalyzer.org), Climate Change Institute, University of Maine, United States.

throughout the combined MFP record, we observe the strong influence of Greenland blocking and North Atlantic SSTs on west GrIS melt rates over annual to decadal time periods.

A multilinear regression analysis quantifies the important contributions from Greenland blocking and North Atlantic SSTs on west GrIS summer temperatures. Using only JJA Denmark Strait SSTs and Z_{500}, a multilinear regression model explains 50% of the Core 6 JJA temperature variance from 1948 to 2013 (pink curve in Figure 3b; $r = 0.70$, $p < 0.001$) and 60% of the Nuuk JJA temperature variance from 1917 to 2013 (light blue curve in Figure 3c; $r = 0.78$, $p < 0.001$).

Despite the strong relationships among North Atlantic SSTs, Greenland blocking and West Greenland temperatures, an additional warming term is critical for producing the anomalously high melt rates since the 1990s. Figure 3 shows that Denmark Strait SSTs and Greenland blocking conditions were nearly identical in the periods 1870–1900 (SST = 10.2°C; Z_{500} = 5,560.4 m) and 1995–2015 (SST = 10.2°C; Z_{500} = 5,552.7 m), yet Nuuk JJA temperatures were 1.2°C warmer in 1995–2015 (6.6°C) than in 1870–1900 (5.4°C). The "missing" 1.2°C warming in the temperature regression model based solely on SST and Z_{500} is represented by the model residual ($T_{Nuuk} - T_{model}$), which has a positive slope over the duration of the record (Figure S5). Site J MFP averaged 22% from 1870 to 1900, compared to 40% in the adjusted Core 1 record from 1995 to 2015 (Figure 3a). Thus, although North Atlantic SSTs and Greenland blocking conditions were very similar in the late 1800s and the early 2000s, a summer warming of ~1.2°C between these periods contributed to a near doubling of MFP in our west GrIS field area. We hypothesize that this additional warming term represents contributions from anthropogenic forcing (Church et al., 2013).

4. Discussion and Conclusions

Our results are consistent with those of Hanna, Jones, et al. (2013) and McLeod and Mote (2015), who similarly find that summertime Greenland blocking events and North Atlantic SSTs are the main drivers of west GrIS meltwater production over annual to decadal time scales. Greenland blocking events became more frequent, and potentially longer in duration, beginning in the 1990s (Figure 3d; McLeod & Mote, 2015), broadly matching the changepoints identified in our ice core MFP records (Figure 1). Anomalously strong blocking has also been identified as the primary cause of the historic 2012 Greenland melting event when 98.6% of the GrIS experienced surface melting (Hanna, Jones, et al., 2013; Nghiem et al., 2012; Tedesco et al., 2013).

It is important to note that Greenland blocking and North Atlantic SSTs are not independent forcing mechanisms, as they have significantly covaried over the instrumental record ($r = 0.54$, $p < 0.05$; 1920–2015 Denmark Strait SST versus Z_{500}). Häkkinen et al. (2011) found more frequent wintertime blocking during AMO positive phases, and the same holds true for the summer. A lag correlation analysis of the low-pass (30-year) filtered JJA AMO index and GBI shows a peak correlation when the AMO leads the GBI by 5 years. This is consistent with the hypothesis that warm-ocean/cool-land conditions favor the formation of blocking highs (Barriopedro et al., 2006; Shabbar et al., 2001), although wind stress anomalies associated with blocking likely feed back to enhance SST anomalies (Häkkinen et al., 2011).

Looking to the future, we hypothesize that 21st century GrIS melt rates over annual to decadal time scales will continue to depend on North Atlantic SSTs and blocking activity; thus, accurate predictions of the AMO and Greenland summer blocking are needed. Our analysis indicates that any future transition to negative AMO conditions (cooler North Atlantic SSTs) with weaker summer blocking would likely provide negative pressure on GrIS summertime temperatures and melt trends for several years or decades. Based on twentieth century observational records and climate model predictions, it has been hypothesized that the AMO will transition into the negative phase in the next 10 to 20 years and return to the positive phase by the 2080s (Chylek et al., 2016; Knight et al., 2005). However, the future behavior of the AMO is highly uncertain because the underlying AMO forcing mechanisms remain debated (Clement et al., 2015) and the AMO response to anthropogenic forcing remains poorly constrained (Klower et al., 2014).

Atmospheric blocking is particularly challenging for global climate models to forecast, and Coupled Model Intercomparison Project Phase 5 models consistently underestimate Atlantic sector blocking frequency and duration since 1950 (Davini & D'Andrea, 2016). Furthermore, the degree to which Arctic amplification (Cohen et al., 2014; Walsh, 2014) and reduced sea ice extent (Liu et al., 2016; McLeod & Mote, 2015) have contributed to the recent increase in summertime Greenland blocking is unclear. In this context, the period of elevated blocking activity from 1870 to 1910 (Figure 3d) is relevant because Arctic sea ice was considerably more extensive in the late nineteenth century than in recent decades (Kinnard et al., 2011).

In summary, the future variability of Greenland blocking and North Atlantic SSTs remain poorly constrained, causing significant uncertainty about future GrIS surface temperatures and melt rates over annual to decadal time scales. However, our analysis indicates that a long-term summertime warming of 1.2°C led to a near doubling of MFP in 1995–2015 compared to 1870–1900, despite nearly identical North Atlantic SSTs and atmospheric blocking activity in the two periods. Thus, additional positive radiative forcing, including from anthropogenic activity, will likely continue to increase temperatures and Greenland melting over multidecadal time scales longer than SST and blocking variability.

Acknowledgments

Data used to create Figures 1 and 2 are available in Data Sets S1–S3 in the supporting information. This project was supported by the U.S. National Science Foundation under grants ARC-1417678 (to E. O. and R. H), ARC-1417921 (to H. M.), ARC-1417640 (to S. B.), and DGE-1313911 (to G. L.). We thank CH2MHill Polar Services, the National Science Foundation Ice Drilling Program Office, and the U.S. Air National Guard 109th Airlift Wing for logistically supporting the GreenTrACS traverse. We also thank two anonymous reviewers for their helpful suggestions and insights.

References

Barriopedro, D., Garcia-Herrera, R., Lupo, A. R., & Hernandez, E. (2006). A climatology of Northern Hemisphere blocking. *Journal of Climate*, *19*(6), 1042–1063. https://doi.org/10.1175/JCLI3678.1

Benson, C. S. (1962). Stratigraphic studies in the snow and firn of the Greenland Ice Sheet, Research Report 70, Snow, Ice and Permafrost Research Establishment.

Box, J. E., Bromwich, D. H., Veenhuis, B. A., Bai, L. S., Stroeve, J. C., Rogers, J. C., et al. (2006). Greenland Ice Sheet surface mass balance variability (1988–2004) from calibrated Polar MM5 output. *Journal of Climate*, *19*(12), 2783–2800. https://doi.org/10.1175/JCLI3738.1

Braithwaite, R. J., Laternser, M., & Pfeffer, W. T. (1994). Variations of near-surface firn density in the lower accumulation area of the Greenland Ice Sheet, Pakitsoq, West Greenland. *Journal of Glaciology*, *40*(136), 477–485. https://doi.org/10.1017/S002214300001234X

Burgess, E. W., Forster, R. R., Box, J. E., Mosley-Thompson, E., Bromwich, D. H., Bales, R. C., & Smith, L. C. (2010). A spatially calibrated model of annual accumulation rate on the Greenland Ice Sheet annual (1958–2007). *Journal of Geophysical Research*, *115*, F02004. https://doi.org/10.1029/2009JF001293

Cappelen J. (2015). Greenland-DMI historical climate data collection 1873–2014—With Danish abstracts. Technical Report No. 15–04, DMI, Copenhagen, Denmark.

Church, J. A., Clark, P. U., Cazenave, A., Gregory, J. M., Jevrejeva, S., Levermann, A., et al. (2013). Sea level change. In T. F. Stocker, et al. (Eds.), *Climate change 2013: The physical science basis. Contribution of Working Group I to the Fifth Assessment Report of the Intergovernmental Panel on Climate Change* (pp. 1137–1216). New York, NY: Cambridge University Press.

Chylek, P., Klett, J. D., Dubey, M. K., & Hengartner, N. (2016). The role of Atlantic Multi-decadal Oscillation in the global mean temperature variability. *Climate Dynamics*, *47*(9–10), 3271–3279. https://doi.org/10.1007/s00382-016-3025-7

Clement, A., Bellomo, K., Murphy, L. N., Cane, M. A., Mauritsen, T., Rädel, G., & Stevens, B. (2015). The Atlantic Multidecadal Oscillation without a role for ocean circulation. *Science*, *350*(6258), 320–324.

Cohen, J., Screen, J. A., Furtado, J. C., Barlow, M., Whittleston, D., Coumou, D., et al. (2014). Recent Arctic amplification and extreme mid-latitude weather. *Nature Geoscience*, *7*(9), 627–637.

Compo, G. P., Whitaker, J. S., Sardeshmukh, P. D., Matsui, N., Allan, R. J., Yin, X., et al. (2011). The Twentieth Century Reanalysis Project. *Quarterly Journal of the Royal Meteorological Society*, *137*(654), 1–28. https://doi.org/10.1002/qj.776

Cox, C., Humphrey, N., & Harper, J. (2015). Quantifying meltwater refreezing along a transect of sites on the Greenland Ice Sheet. *The Cryosphere*, *9*(2), 691–701. https://doi.org/10.5194/tc-9-691-2015

Davini, P., & D'Andrea, F. (2016). Northern Hemisphere atmosphere blocking representation in global climate models: Twenty years of improvements. *Journal of Climate Dynamics*, *29*(24), 8823–8840. https://doi.org/10.1175/JCLI-D-16-0242.1

De la Peña, S., Howat, I. M., Nienow, P. W., van den Broeke, M. R., Mosley-Thompson, E., Price, S. F., et al. (2015). Changes in the firn structure of the western Greenland Ice Sheet caused by recent warming. *The Cryosphere*, *9*(3), 1203–1211. https://doi.org/10.5194/tc-9-1203-2015

Enderlin, E. M., Howat, I. M., Jeong, S., Noh, M.-J., van Angelen, J. H., & van den Broeke, M. R. (2014). An improved mass budget for the Greenland Ice Sheet. *Geophysical Research Letters*, *41*, 866–872. https://doi.org/10.1002/2013GL059010

Fettweis, X., Box, J. E., Agosta, C., Amory, C., Kittel, C., & Gallée, H. (2016). Reconstructions of the 1900–2015 Greenland Ice Sheet surface mass balance using the regional climate MAR model. *The Cryosphere Discussions*, 1–32. https://doi.org/10.5194/tc-2016-268

Fettweis, X., Franco, B., Tedesco, M., van Angelen, J. H., Lenaerts, J. T. M., van den Broeke, M. R., & Gallée, H. (2013). Estimating the Greenland Ice Sheet surface mass balance contribution to future sea level rise using the regional atmospheric climate model MAR. *The Cryosphere*, *7*(2), 469–489. https://doi.org/10.5194/tc-7-469-2013

Häkkinen, S., Rhines, P. B., & Worthen, D. L. (2011). Atmospheric blocking and Atlantic multidecadal ocean variability. *Science*, *334*(6056), 655–659. https://doi.org/10.1126/science.1205683

Hanna, E., Jones, J. M., Cappelen, J., Mernild, S. H., Wood, L., Steffen, K., & Huybrechts, P. (2013). The influence of North Atlantic atmospheric and oceanic forcing effects on 1900–2010 Greenland summer climate and ice melt/runoff. *International Journal of Climatology*, *33*(4), 862–880. https://doi.org/10.1002/joc.3475

Hanna, E., Mernild, S. H., Cappelen, J., & Steffen, K. (2012). Recent warming in Greenland in a long-term instrumental (1881–2012) climate context: I. Evaluation of surface air temperature records. *Environmental Research Letters*, *7*(4), 045404. https://doi.org/10.1088/1748-9326/7/4/045404

Hanna, E., Navarro, F. J., Pattyn, F., Domingues, C. M., Fettweis, X., & Ivins, E. R. (2013). Ice-sheet mass balance and climate change. *Nature*, *498*(7452), 51–59. https://doi.org/10.1038/nature12238

Harper, J., Humphrey, N., Pfeffer, W. T., Brown, J., & Fettweis, X. (2012). Greenland ice-sheet contribution to sea-level rise buffered by meltwater storage in firn. *Nature*, *491*(7423), 240–243. https://doi.org/10.1038/nature11566

Humphrey, N. F., Harper, J. T., & Pfeffer, W. T. (2012). Thermal tracking of meltwater retention in Greenland's accumulation area. *Journal of Geophysical Research*, *117*, F01010. https://doi.org/10.1029/2011JF002083

Jaffrezo, J. L., Davidson, C. I., Legrand, M., & Dibb, J. E. (1994). Sulfate and MSA in the air and snow on the Greenland Ice Sheet. *Journal of Geophysical Research*, *99*, 11,241–11,253. https://doi.org/10.1029/93JD02913

Kameda, T., Narita, H., Shoji, H., Nisho, F., Fujii, Y., & Watanabe, O. (1995). Melt features in ice cores from Site J, southern Greenland: Some implications for summer climate since AD 1550. *Annals of Glaciology*, *21*, 51–58. https://doi.org/10.1017/S0260305500015597

Kerr, R. A. (2000). A North Atlantic climate pacemaker for the centuries. *Science*, *288*(5473), 1984–1985. https://doi.org/10.1126/science.288.5473.1984

Killick, R., Fearnhead, P., & Eckley, I. A. (2012). Optimum detection of changepoints with a linear computational cost. *Journal of the American Statistical Association*, *107*(500), 1590–1598. https://doi.org/10.1080/01621459.2012.737745

Kinnard, C., Zdanowicz, C. M., Fisher, D. A., Isaksson, E., de Vernal, A., & Thompson, L. G. (2011). Reconstructed changes in Arctic sea ice over the past 1,450 years. *Nature*, *479*(7374), 509–512. https://doi.org/10.1038/nature10581

Klower, M., Latif, M., Ding, H., Greatbatch, R., & Park, W. (2014). Atlantic meridional overturning circulation and the prediction of North Atlantic sea surface temperature. *Earth and Planetary Science Letters*, *406*, 1–6. https://doi.org/10.1016/j.epsl.2014.09.001

Knight, J. R., Allan, R. J., Folland, C. K., Vellinga, M., & Mann, M. E. (2005). A signature of persistent natural thermohaline circulation cycles in observed climate. *Geophysical Research Letters*, *32*, L20708. https://doi.org/10.1029/2005GL024233

Li, J., & Zwally, H. J. (2011). Modeling of firn compaction for estimating ice-sheet mass change from observed ice-sheet elevation change. *Annals of Glaciology*, *52*(59), 1–7. https://doi.org/10.3189/172756411799096321

Liu, J. P., Chen, Z. Q., Francis, J., Song, M. R., Mote, T., & Hu, Y. Y. (2016). Has Arctic sea ice loss contributed to increased surface melting of the Greenland Ice Sheet? *Journal of Climatology*, *29*(9), 3373–3386. https://doi.org/10.1175/JCLI-D-15-0391.1

Machguth, H., MacFerrin, M., van As, D., Box, J. E., Charalampidis, C., Colgan, W., et al. (2016). Greenland meltwater storage in firn limited by near-surface ice formation. *Nature Climate Change*, *6*(4), 390–393. https://doi.org/10.1038/nclimate2899

McLeod, J. T., & Mote, T. L. (2015). Linking interannual variability in extreme Greenland blocking episodes to the recent increase in summer melting across the Greenland Ice Sheet. *International Journal of Climatology*, *36*, 1484–1499.

Mernild, S. H., Hanna, E., Yde, J. C., Cappelen, J., & Malmros, J. K. (2014). Coastal Greenland air temperature extremes and trends 1890–2010: Annual and monthly analysis. *International Journal of Climatology*, *34*(5), 1472–1487. https://doi.org/10.1002/joc.3777

Moore, J. C., Grinsted, A., Kekonen, T., & Pohjola, V. (2005). Separation of melting and environmental signals in an ice core with seasonal melt. *Geophysical Research Letters*, *32*, L10501. https://doi.org/10.1029/2005GL023039

Mosley-Thompson, E., McConnell, J. R., Bales, R. C., Li, Z., Lin, P. N., Steffen, K., et al. (2001). Local to regional-scale variability of annual net accumulation on the Greenland Ice Sheet from PARCA cores. *Journal of Geophysical Research*, *106*(D24), 33,839–33,851. https://doi.org/10.1029/2001JD900067

Mote, T. L. (1998). Mid-tropospheric circulation and surface melt on the Greenland Ice Sheet. Part I: Atmospheric teleconnections. *International Journal of Climatology*, *18*(2), 111–129. https://doi.org/10.1002/(SICI)1097-0088(199802)18:2%3C111::AID-JOC227%3E3.0.CO;2-X

Mote, T. L. (2007). Greenland surface melt trends 1973–2007: Evidence of a large increase in 2007. *Geophysical Research Letters*, *34*, L22507. https://doi.org/10.1029/2007GL031976

Nghiem, S., Hall, D., Mote, T., Tedesco, M., Albert, A., Keegan, K., et al. (2012). The extreme melt across the Greenland Ice Sheet in 2012. *Geophysical Research Letters*, *39*, L20502. https://doi.org/10.1029/2012GL053611

Osterberg, E. C., Handley, M. J., Sneed, S. B., Mayewski, P. A., & Kreutz, K. J. (2006). Continuous ice core melter system with discrete sampling for major ion, trace element, and stable isotope analyses. *Environmental Science and Technology*, *40*(10), 3355–3361. https://doi.org/10.1021/es052536

Osterberg, E. C., Hawley, R. L., Wong, G., Kopec, B., Ferris, D., & Howley, J. (2015). Coastal ice-core record of recent northwest Greenland temperature and sea-ice concentration. *Journal of Glaciology*, *61*(230), 1137–1146. https://doi.org/10.3189/2015JoG15J054

Pfeffer, W. T., & Humphrey, N. F. (1998). Formation of ice layers by infiltration and refreezing of meltwater. *Annals of Glaciology*, *26*, 83–91. https://doi.org/10.1017/S0260305500014610

Pohjola, V. A., Moore, J. C., Isaksson, E., Jauhiainen, T., van de Wal, R. S. W., Martma, T., et al. (2002). Effect of periodic melting on geochemical and isotopic signals in an ice core from Lomonosovfonna, Svalbard. *Journal of Geophysical Research*, *107*(D4), 4036. https://doi.org/10.1029/2000JD000149

Sasgen, I., van den Broeke, M., Bamber, J. L., Rignot, E., Sørensen, L. S., Wouters, B., et al. (2012). Timing and origin of recent regional ice-mass loss in Greenland. *Earth and Planetary Science Letters*, *333*, 293–303.

Shabbar, A., Huang, J., & Higuchi, K. (2001). The relationship between the wintertime North Atlantic Oscillation and blocking episodes in the North Atlantic. *International Journal of Climatology*, *21*(3), 355–369. https://doi.org/10.1002/joc.612

Sørensen, L. S., Simonsen, S. B., Nielsen, K., Lucas-Picher, P., Spada, G., Adalgeirsdottir, G., et al. (2011). Mass balance of the Greenland Ice Sheet (2003–2008) from ICESat data—The impact of interpolation, sampling and firn density. *The Cryosphere*, *5*(1), 173–186. https://doi.org/10.5194/tc-5-173-2011

Tedesco, M., Fettweis, X., Mote, T., Wahr, J., Alexander, P., Box, J. E., & Wouters, B. (2013). Evidence and analysis of 2012 Greenland records from spaceborne observations, a regional climate model and reanalysis data. *The Cryosphere*, *7*(2), 615–630. https://doi.org/10.5194/tc-7-615-2013

van Angelen, J. H., Lenaerts, J. T. M., van den Broeke, M. R., Fettweis, X., & van Meijgaard, E. (2013). Rapid loss of firn pore space accelerates 21st century Greenland mass loss. *Geophysical Research Letters*, *40*, 2109–2113. https://doi.org/10.1002/grl.50490

van Angelen, J. H., van den Broeke, M. R., Wouters, B., & Lenaerts, J. T. M. (2014). Contemporary (1960–2012) evolution of the climate and surface mass balance of the Greenland Ice Sheet. *Surveys of Geophysics*, *35*(5), 1155–1174. https://doi.org/10.1007/s10712-013-9261-z

van den Broeke, M. R., Enderlin, E. M., Howat, I. M., Kuipers, M., Noël, B., van de Berg, W. J., et al. (2016). On the recent contribution of the Greenland Ice Sheet to sea level change. *The Cryosphere*, *10*(5), 1933–1946. https://doi.org/10.5194/tc-10-1933-2016

Walsh, J. E. (2014). Intensified warming of the Arctic: Causes and impacts on middle latitudes. *Global and Planetary Change*, *117*, 52–63. https://doi.org/10.1016/j.gloplacha.2014.03.003